Superconducting-normal metal interfaces produced by reactive ion etching

K. Lin, Y. K. Kwong, M. Park, J. M. Parpia, and M. S. Isaacson
School of Applied and Engineering Physics and Laboratory of Atomic and Solid State Physics, Clark Hall, Cornell University, Ithaca, New York 14853

(Received 29 May 1991; accepted 23 July 1991)

We have used CHF_3/O_2 reactive ion etching to reliably change the superconducting transition temperature (T_c) of aluminum thin films by 10–50 mK. Microanalyses using scanning Auger and scanning electron microscopy (SEM) indicate that the etching process results in a surface layer of high fluorine and low oxygen contents. The analyses show that photolithography and etching can produce very sharp interfaces between etched (lowered T_c) and unetched (higher T_c) regions. This technique is applied to study two specific configurations. First, long strips of aluminum thin films are patterned with a periodic structure of alternating regions of high and low T_c. The resistive transition of these films shows a surprisingly long proximity effect with a length scale of more than 50 μm, nearly two orders of magnitude greater than expected from established theory. Second, an aluminum strip with a single *S–N–S* (high–low–high T_c) structure possesses a resistive anomaly just above the lower T_c. This anomaly depends on the position of the measurement voltage probes relative to the interfaces and appears to have a length scale of several μm.

I. INTRODUCTION

In a previous study,[1] we noted that reactive ion etching (RIE) of aluminum thin films using CHF_3/O_2 gases can reproducibly shift the superconducting transition temperature T_c by 30–40 mK. This suggests a method in which lithography and RIE are combined to create arbitrary regions of high and low T_c within a single continuous film, as shown schematically in Fig. 1(a). We are motivated by the possibility of using such films as valid equivalents or models of inhomogeneous and anisotropic superconducting systems such as superlattices and superconductor–normal metal–superconductor (*S–N–S*) junctions. Traditional methods of fabricating such systems involve sequential deposition of two or more different materials.[2,3] Typical problems include interlayer diffusion, island formation, and contamination. Even though our films are strictly two-dimensional with respect to superconductivity, the physics of inhomogeneity and anisotropy in thin films is expected to be similar to that of three-dimensional systems.

The main criterion that we must demonstrate is that the films have well-defined regions of different T_c's and the boundaries are sufficiently sharp so that the physics studied is not compromised. We used both microanalysis performed by scanning Auger microscopy (SAM) and scanning electron microscopy (SEM), and low-temperature measurements to demonstrate that these criteria are met consistently in our films. Our 2D analog of a superlattice is the periodically etched film shown schematically in Fig. 1(a).[4] The flexibility of the fabrication method permits us to study a wide range of relative lengths and periods, and their relation to superconducting properties. Our version of an *S–N–S* structure with corresponding voltage probes is shown in Fig. 1(b).[5] Following conventional definitions, "normal metal" (*N*) is used to indicate a superconductor above its transition temperature. The multiple voltage probes placed at varying distances from the etch boundaries allow us to study the potentials associated with the *S–N* interface over a small length scale.

II. SAMPLE FABRICATION

All our films are 25-nm-thick aluminum deposited by thermal evaporation in a base vacuum of $< 3 \times 10^{-6}$ Torr at

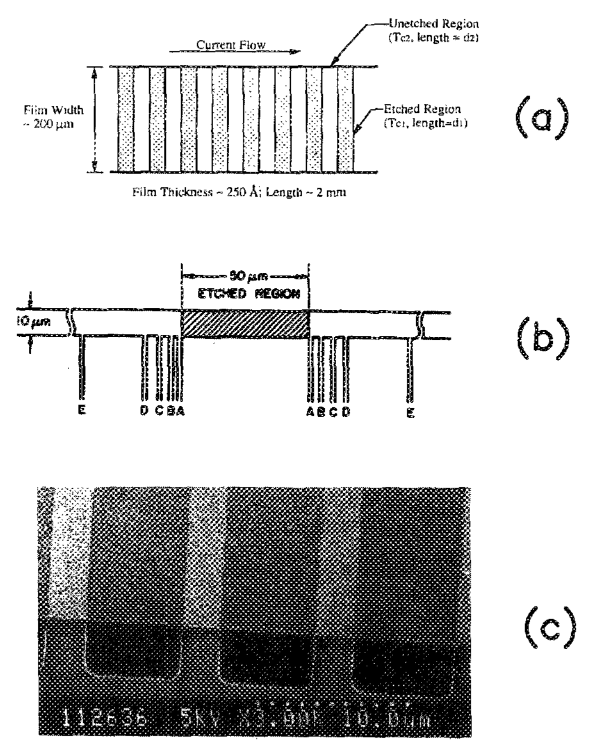

FIG. 1. (a) Schematic drawing of an aluminum thin-film strip with periodically modulated T_c. (b) Schematic of an aluminum thin film with a single etched section, with symmetrically placed electrodes A–E. (c) SEM micrograph of the grating structure in (a), showing the sharp boundaries between unetched and etched sections.

rates of 15–20 Å/s. The aluminum film strips along with voltage and current pads and leads are defined by photolithography and liftoff. The substrate is a LPCVD silicon nitride film deposited on a silicon wafer. Etch patterns in the aluminum film are then defined by a second photolithography step using a GCA DSW4800 10:1 stepper. In this step, a thin (≈ 300 Å) coat of PMMA is spun onto the wafer before the photoresist to protect the thin aluminum films from the metallic hydroxide photoresist developer. For the RIE, we use a Materials Research Corp. 720 Magnetron Ion Etcher. The machine has a magnetically confined plasma providing uniform etching conditions over a 3-in. wafer, which sits on a holder cooled by a helium gas–water interface. A quick 15-s O_2 plasma first removes the PMMA coating in the exposed area, then the aluminum film underneath is etched in the CHF_3/O_2 plasma. The etching parameters are: CHF_3/O_2 gases at 30 sccm flow rate, 1 kW total incident power, and 20 s etching time. We note that this is an efficient recipe for etching silicon nitride, but it does not result in the removal of any aluminum. Therefore, when we refer to the RIE of aluminum thin films, we actually mean that the film was exposed to the RIE plasma. After etching, the resist coatings are removed in solvents.

The etching typically changes the RRR (ratio of resistance at room temperature to that at 4.2 K) by 0.5%, the sheet resistance by $< 10\%$, and the electronic diffusion constant by 20%. Our previous study[1] has also shown that RIE does not change the low-temperature electronic transport properties in any significant way.

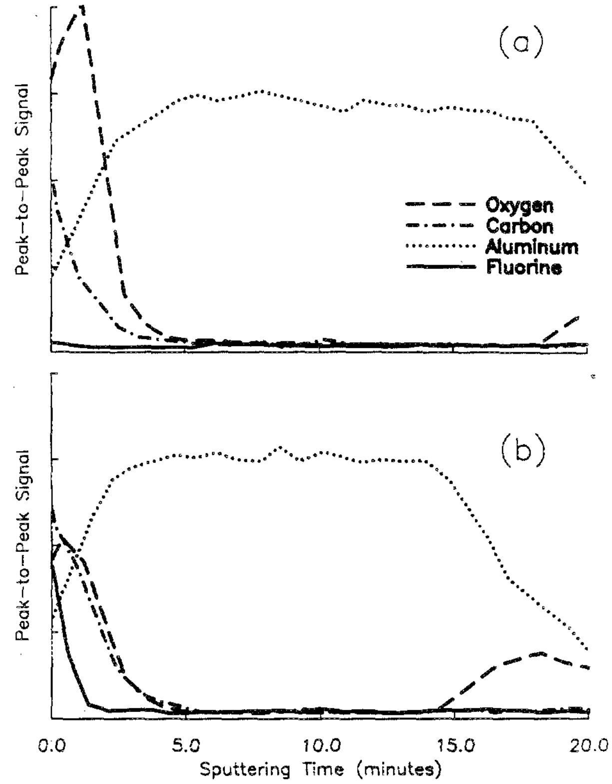

FIG. 2. Auger depth profile for peak-to-peak signals of aluminum, carbon, oxygen, and fluorine for unetched (a) and etched (b) aluminum thin films. The carbon signal is probably due to a small contamination layer accumulated in the microprobe vacuum chamber.

III. MICROANALYSIS

Two relevant questions regarding this technique are: how are the T_c's modified, and how sharp are the boundaries between unetched and etched regions? The T_c of a superconducting aluminum thin film is very sensitive to many factors, such as purity, substrate, grain size, oxide formation, and surface and deposition conditions. RIE may modify one or more of these factors. Without an exhaustive and systematic study, it is nearly impossible to attribute the T_c change to any one cause. For example, in our previous study,[1] we performed the RIE using the same gases but in a different machine. There, the RIE *raised* the T_c of aluminum films. In the current study, the RIE *lowers* the T_c. In spite of the very different etching properties of the two etchers, the reason for their different effects on T_c is not obvious, but clearly depends on the exact process conditions. A systematic study would be quite time consuming. For this study, it is sufficient to note that the physics of interest depends upon the T_c differences, not on how they are achieved. The exact mechanism will be investigated in the future.

The question of the sharpness of the boundaries is much more relevant to our study. If the boundaries between unetched and etched regions should somehow be blurred or smeared over a significant length scale, we would have created a problem analogous to interlayer diffusion in superlattices. Figures 2(a) and 2(b) show the Auger depth profile of unetched and etched aluminum films for oxygen, fluorine, carbon, and aluminum. The etched film surface is characterized by a surface layer of fluorine-rich material. The surface fluorine signal disappears after baking the film at 300 °C overnight, indicating that the fluorine species are weakly bound on the surface. The etched sections also have a depleted oxygen signal relative to the unetched sections. Figure 3 shows line scans of fluorine and oxygen peak signals across several periods of the grating structure shown in Fig. 1(a). The signals consistently reflect the periodic structures patterned by photolithography. The signal drops from 90% to 10% of maximum over a distance of about 2 μm, the estimated spot size of the Auger microprobe used in this study (Physical Electronics PHI-590). Figure 1(c) is an SEM micrograph of the edge of a periodically etched aluminum film. We speculate that the enhanced oxygen concentration in the unetched regions might be responsible for the contrast between the etched and unetched regions. The micrograph demonstrates the uniformity of the different sections and the very sharp boundaries. Thus the boundaries appear to be sharply defined to at least 0.1 μm, much shorter than the length scales that appeared in the phenomena that we describe in the following sections.

IV. LONG-RANGE SUPERCONDUCTING PROXIMITY EFFECT

The sample film strips used in this study are shown schematically in Fig. 1(a). Each sample chip that is cooled down to liquid helium temperatures contains 16 such strips having

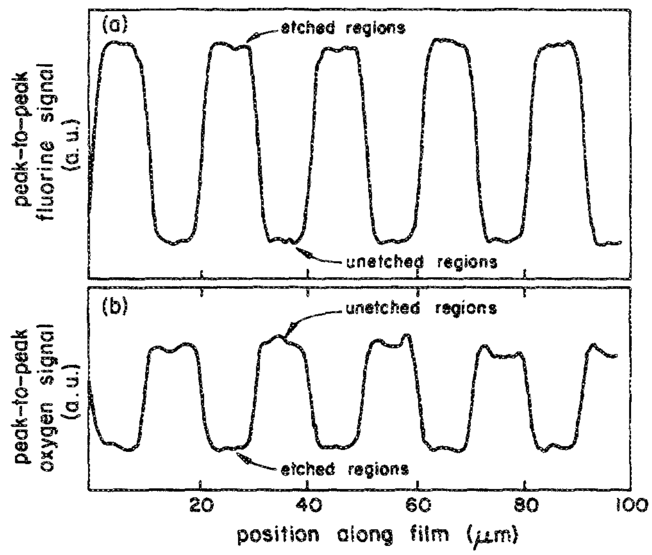

FIG. 3. Line scan tracing the fluorine (a) and oxygen (b) Auger peak signals across several periods of etched and unetched aluminum film sections. The resolution is limited by the electron probe size, estimated to be around 2 μm.

varying values of d_1 and d_2 together with completely unetched and etched control sections. Note that the quoted values of d_1 and d_2 are the *designed* lengths. The actual value after lithography may differ by ± 0.2 μm in a systematic way. This error is only significant for the smallest periods. We measure the resistive transitions with a four-terminal ac resistance bridge operating at 17 Hz. T_c is defined as the temperature where the resistance drops to half the normal state value.

In the limit of small periodicity, $\Lambda \equiv d_1 + d_2 \to 0$, one expects the film strip to have one single continuous transition, behaving like a single homogeneous superconductor. In the opposite limit, $\Lambda \to \infty$, the transition should have two distinct parts at the higher and lower T_c's, behaving as two different superconductors in series. A crossover from the first behavior to the second should occur at a characteristic length of the system. A relevant length is the Ginzburg–Landau (GL) coherence length which is the length over which the GL superconducting wave function varies.[6] Figure 4(b) plots the resistive transitions of strips with $d_1 = d_2$, showing the gradual shift from single transition to two discrete ones as Λ increases. The surprising fact is the extremely long length scale over which the single transition is preserved. The data demonstrate a proximity effect extending over a length of more than 50 μm. This is an order of magnitude longer than all known transport length scales in aluminum thin films. The GL coherence length at 10 mK above T_{c1} is about 1 μm, and the inelastic diffusion length is no more than 10 μm. Other possibly applicable lengths are similarly much less than 50 μm.[4]

The T_c depend only weakly on Λ as shown in Fig. 4(a). But the T_c does depend strongly and monotonically on the ratio d_1/d_2. Using linearized Ginzburg–Landau theory, with the additional assumption of the coherence length $\ll \Lambda$, we can fit the measured T_c to the expression:[3]

$$\frac{\Delta T_c}{T_c - T_{c1}} = 1 + p\frac{d_1}{d_2}, \quad (1)$$

where p is a factor of order unity characterizing the boundary conditions. Figure 5 shows fits of this equation to three different samples. The large error bars on two points reflect the aforementioned lithographic uncertainty for small values of d_1 or d_2. The equation works remarkably well. Since the condition of coherence length being $\ll \Lambda$ is not expected to be true for our films, these results again suggest the presence of a very long length scale of yet unknown origin. Further details are discussed elsewhere.[4]

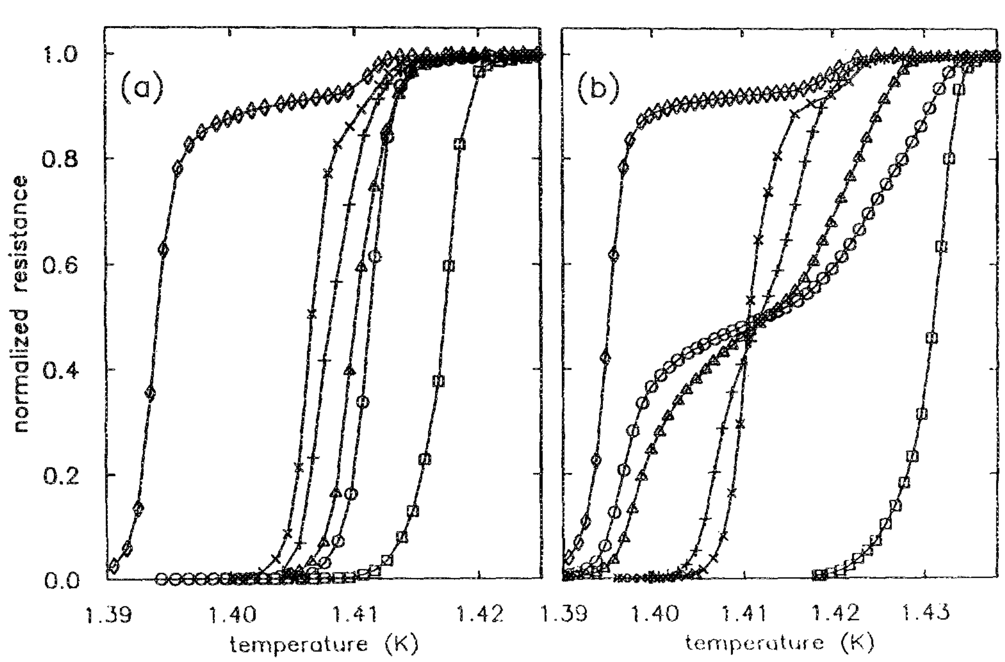

FIG. 4. Typical superconducting resistive transitions of two different aluminum films with periodically modulated T_c. In both (a) and (b), $d_1 = d_2$, and ◇ and □ are the uniformly etched and unetched films. In (a), ×, +, Δ, and ○ represent $\Lambda = 4$, 10, 20, and 100 μm, respectively. In (b), the same symbols represent $\Lambda = 20$, 100, 200, and 400 μm.

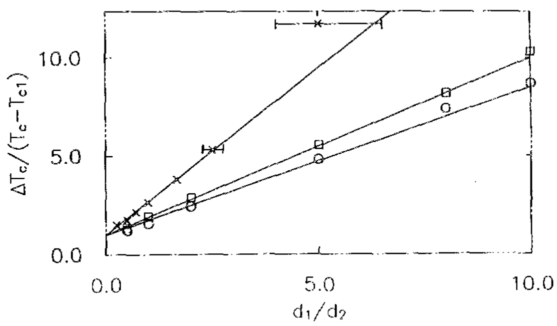

FIG. 5. Data for three different films, reduced according to Eq. (1). Solid lines are least-square fits using p as the fitting parameter.

V. RESISTIVE ANOMALY IN SINGLE *S–N–S* STRUCTURES

Several experiments have attempted to investigate the spatial dependence of the potentials in a superconducting film in the vicinity of a phase slip center.[7,8] These results, along with the long-range proximity effect reported above, prompted us to investigate samples with single superconducting–normal–superconducting (*S–N–S*) structures. We report here an anomalous peak observed in the resistive transition of these samples, for which the peak resistance is *greater* than the normal state value.

The samples are patterned aluminum films with a thickness of 25 nm, a width of 10 μm, and a total length of 2 mm. A schematic of a typical sample is shown in Fig. 1(b). The voltage leads are located symmetrically about a central 50-μm-long section which has been exposed to RIE. In the sample of Fig. 1(b), the etch suppresses the T_c of the central region by $\approx$45 mK. The films are relatively clean, with residual resistance ratio >3 and diffusion constant >70 cm^2/s. The 2-μm-wide voltage leads were placed at 0, 4, 9, 16, and 50 μm from each of the two *N–S* interfaces and are designated as A through E, respectively. Other samples investigated have pairs of voltage leads located within the etched regions, and the resistive transitions measured by these leads show no anomaly.

The resistive transitions as measured across voltage pairs A through E are shown in Figs. 6(a) and 6(b). In Fig. 6(a), we show the measured resistance across pairs of symmetrically placed leads. The resistance of the outermost pair, E, decreases rapidly by about one-third of its value and then decreases gradually by another one-third before the etched region undergoes its superconducting transition. This behavior is consistent with the resistive transition of two materials with similar T_c's in series with each other, with a long length scale proximity effect. The resistance of the innermost pairs of voltage leads (paris A and B) exhibits the anomalous behavior. In Fig. 6(a), the resistance of pair A is constant with decreasing temperature until $\approx$1.34 K, where it increases by about 5% and then rejoins the other curves. Further, the resistance across pair B displays a similar (though smaller) anomaly of about 3% of the normal resistance. The absolute magnitude of the resistance increase observed with pair A is larger than that with pair B.

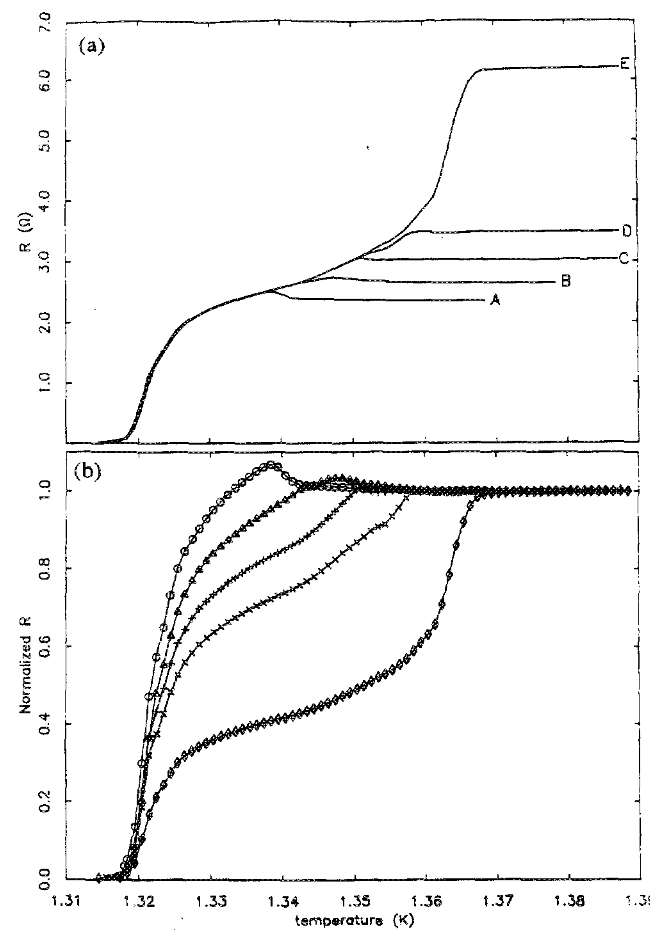

FIG. 6. (a) Resistive transitions as measured by voltage probe pairs A through E, schematically shown in Fig. 1(b). The central etched region have T_c 45 mK lower than the adjacent unetched film. (b) The same curves normalized to resistance at 1.39 K. O, Δ, $+$, $\times$, and $\Diamond$ represent voltage pairs A, B, C, D, and E, respectively. The anomaly is clearly observable for pairs A and B.

These details are more easily observed in the plots [see Fig. 6(b)] of the resistance normalized to its values at 1.39 K. Here, it is clear that only the innermost pairs of leads (pairs A and B) exhibit the anomalous behavior. Studies with *etched* (normal) probes, usually located within the etched region, do not exhibit this anomaly. Likewise, no anomaly is present for samples whose etched and unetched regions have T_c difference less than $\approx$30 mK. The last situation would result in the absence of any well-defined *N–S* interface in the presence of the long-range proximity effect described in Sec. IV. Thus, the resistive anomaly is observable over a characteristic length scale of a few microns and is clearly associated with the superconducting potential in the presence of *N–S* interfaces. The application of a small magnetic field (>10 G) quenches this peak. The peak magnitude is not dependent on excitation current.

The significance of a number of mechanisms can be excluded. For example, Andreev scattering and fluctuations in the phase of the order parameter may give rise to a voltage, but they cannot produce a resistance above the normal state value. Yet, although the anomaly seems surprising at first sight, we believe it is consistent with a nearly constant superconducting potential near a N–S interface. Further details are discussed elsewhere.[5]

VI. CONCLUSIONS

In this paper, we have demonstrated the considerable flexibility of our processing technique. Microanalysis and low-temperature measurements have shown the consistent quality of the RIE processed aluminum films. The long-range proximity effect observed in periodically modulated T_c strips and the resistive anomaly in S–N–S structures have revealed new physics of boundary effects. These systems offer many possibilities for further study. The use of different superconducting materials should tell us whether these observations are unique to aluminum. Alternate ways of modifying the thin film can provide different characteristic changes. For example, ion milling can physically remove material, and ion implantation can induce bulk damage in addition to simple surface modification. Electron-beam lithography can also be used if finer scale structures are required, without significant change of the present processing method.

ACKNOWLEDGMENTS

The authors thank P. Hakonen and R. A. Buhrman for helpful discussions. We also thank L. Rathbun and P. Chapman for help with the Auger analyses. This research is supported by AFSOR Grant No. 90-0111, and the Cornell Materials Science Center under NSF Grant No. DMR-88-18558. All fabrication work was performed at the Cornell National Nanofabrication Facility supported under NSF Grant No. ECS-8619094.

[1]Y. K. Kwong, K. Lin, P. Hakonen, J. M. Parpia, and M. Isaacson, J. Vac. Sci. Technol. B **7**, 2020 (1989).

[2]J. Clarke, in *Nonequilibrium Superconductivity*, edited by D. N. Langenberg and A. I. Larkin (Elsevier, New York, 1986).

[3]B. Y. Jin and J. B. Ketterson, Adv. Phys. **38**, 189 (1989).

[4]Y. K. Kwong, K. Lin, M. Isaacson, and J. M. Parpia, Phys. Rev. Lett. **65**, 2905 (1990).

[5]Y. K. Kwong, K. Lin, P. J. Hakonen, J. M. Parpia, and M. S. Isaacson, Phys. Rev. B **44**, 462 (1991).

[6]M. Tinkham, *Introduction to Superconductivity* (Krieger, Malabar, FL, 1980).

[7]G. J. Dolan and L. D. Jackel, Phys. Rev. Lett. **39**, 1628 (1977).

[8]W. J. Skocpol and L. D. Jackel, Physica B/C **108**, 1021 (1981).